



HAL
open science

Sensitivity of chemical species to climatic changes in the last 45 kyr as revealed by high-resolution Dome C (East Antarctica) ice-core analysis

Roberto Udisti, Silvia Becagli, Silvia Benassai, Martine de Angelis, Margareta Hansson, Jean Jouzel, Jacob Schwander, Jørgen Steffensen, Rita Traversi, Eric Wolff

► To cite this version:

Roberto Udisti, Silvia Becagli, Silvia Benassai, Martine de Angelis, Margareta Hansson, et al.. Sensitivity of chemical species to climatic changes in the last 45 kyr as revealed by high-resolution Dome C (East Antarctica) ice-core analysis. *Annals of Glaciology*, 2004, 39, pp.457-466. 10.3189/172756404781814096 . hal-03220137

HAL Id: hal-03220137

<https://hal.science/hal-03220137>

Submitted on 7 May 2021

HAL is a multi-disciplinary open access archive for the deposit and dissemination of scientific research documents, whether they are published or not. The documents may come from teaching and research institutions in France or abroad, or from public or private research centers.

L'archive ouverte pluridisciplinaire **HAL**, est destinée au dépôt et à la diffusion de documents scientifiques de niveau recherche, publiés ou non, émanant des établissements d'enseignement et de recherche français ou étrangers, des laboratoires publics ou privés.



Distributed under a Creative Commons Attribution 4.0 International License

Sensitivity of chemical species to climatic changes in the last 45 kyr as revealed by high-resolution Dome C (East Antarctica) ice-core analysis

Roberto UDISTI,¹ Silvia BECAGLI,¹ Silvia BENASSAI,¹ Martine DE ANGELIS,² Margareta E. HANSSON,³ Jean JOUZEL,⁴ Jacob SCHWANDER,⁵ Jørgen P. STEFFENSEN,⁶ Rita TRAVERSI,¹ Eric WOLFF⁷

¹Department of Chemistry, University of Florence, Via della Lastruccia 3, I-50019 Sesto F.no (Florence), Italy
E-mail: udisti@unifi.it

²Laboratoire de Glaciologie et Géophysique de l'Environnement du CNRS, 54 rue Molière, BP 96, 38402 Saint-Martin-d'Hères Cedex, France

³Department of Physical Geography and Quaternary Geology, Stockholm University, S-106 91 Stockholm, Sweden

⁴Laboratoire des Sciences du Climat et de l'Environnement, UMR CEA-CNRS, 91191 Gif-sur-Yvette, France

⁵Physics Institute, University of Bern, Sidlerstrasse 5, CH-3012 Bern, Switzerland

⁶Department of Geophysics, The Niels Bohr Institute, University of Copenhagen, Juliane Maries Vej. 30, DK-2100 Copenhagen, Denmark

⁷British Antarctic Survey, Natural Environment Research Council, Madingley Road, Cambridge CB3 0ET, UK

ABSTRACT. To assess the cause/effect relationship between climatic and environmental changes, we report high-resolution chemical profiles of the Dome C ice core (788 m, 45 kyr), drilled in the framework of the European Project for Ice Coring in Antarctica (EPICA). Snow-concentration and depositional-flux changes during the last deglaciation were compared with climatic changes, derived by δD profile. Concentration and temperature profiles showed an anticorrelation, driven by changes in source intensity and transport efficiency of the atmospheric aerosol and by snow accumulation-rate variations. The flux calculation allowed correction for accumulation rate. While sulphate and ammonium fluxes are quite constant, Na^+ , Mg^{2+} and Ca^{2+} underwent the greatest changes, showing fluxes respectively about two, three and six times lower in the Holocene than in the Last Glacial Maximum. Chloride, nitrate and methanesulphonic acid (MSA) also exhibited large changes, but their persistence depends on depositional and post-depositional effects. The comparison between concentrations and δD profiles revealed leads and lags between chemical and temperature trends: Ca^{2+} and nitrate preceded by about 300 years the δD increase at the deglaciation onset, while MSA showed a 400 year delay. Generally, all components reached low Holocene values in the first deglaciation step (18.0–14.0 kyr BP), but Na^+ , Mg^{2+} and nitrate show changes during the Antarctic Cold Reversal (14.0–12.5 kyr BP).

1. INTRODUCTION

The interactions between climate changes and environmental variations are complex and their cause/effect relationship is not yet fully understood. Indeed, if the large glacial/interglacial changes in the Earth climate system are attributed to orbital driving forces (see, e.g., Petit and others, 1999), the role played by environmental changes (e.g. sea level, ice cover, aerosol production) in fast climate changes through feedback processes is still an open question. Polar ice cores constitute a conservative and reliable environmental archive storing the gas and aerosol composition of the atmosphere for hundreds of thousands of years, and ice cores are widely used to reconstruct climatic and environmental changes over several glacial/interglacial cycles (Petit and others, 1999). While stable-isotopic profiles (δD or $\delta^{18}O$, deuterium excess) provide a reliable reconstruction of climatic conditions (temperature and relative humidity) in the deposition-site and moisture-source areas (Jouzel and others, 1995; Stenni and others, 2001; Vimeux and others, 2002) and can be used to evaluate accumulation rates (Schwander and others, 2001), selected chemical

compounds have been proposed as actual or potential markers of environmental changes. For instance, atmospheric load of dust and sea-salt components, mainly related to atmospheric circulation processes, were inferred from the Ca^{2+} and Na^+ content (Legrand and others, 1988; Steig and others, 2000; Röthlisberger and others, 2002a; Ruth and others, 2002), marine biogenic activity from methanesulphonic acid (MSA) and non-sea-salt sulphate ($nssSO_4^{2-}$) (Legrand and others, 1991, 1997; Hansson and Saltzman, 1993), continental biogenic changes from ammonium (Dentener and Crutzen, 1994; Legrand and others, 1998), N-cycle compounds transformation and transport processes from nitrate (Mayewski and Legrand, 1990; Wolff, 1995) and volcanic activity from non-biogenic sulphuric acid (Delmas and others, 1992; Cole-Dai and others, 2000; Udisti and others, 2000; Zielinski, 2000).

In this paper, we compare the high-resolution chemical profiles of several ionic components (main and trace anions and cations) with δD and electrical conductivity measurement (ECM) profiles, all measured along the first EPICA (European Project for Ice Coring in Antarctica) Dome C ice core (EDC96). The chemical profiles constitute a continuous

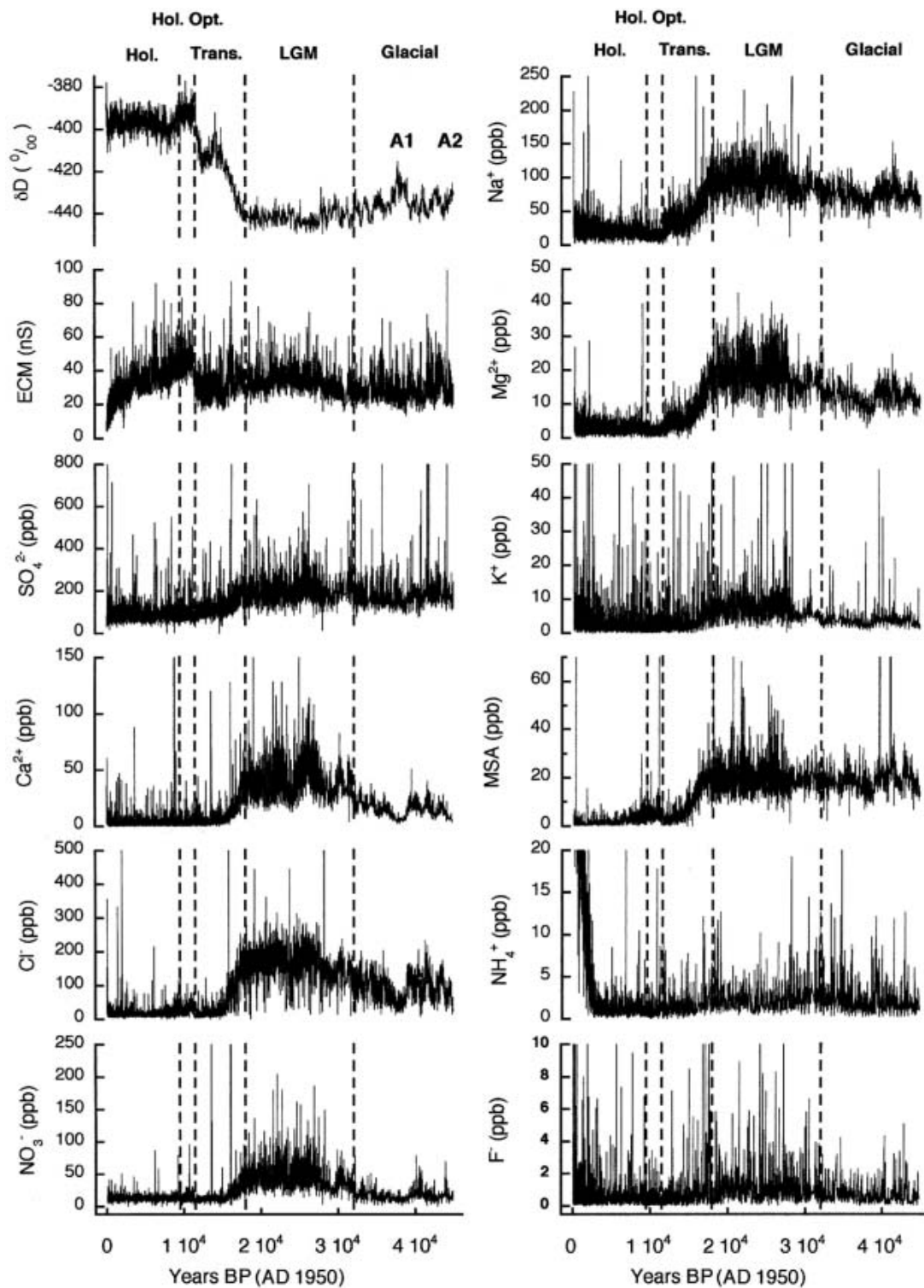


Fig. 1. Stratigraphic profiles of the analyzed chemical species along the EDC96 ice core. Dashed vertical lines represent the borders between the climatic periods discussed.

high-resolution record spanning the last 45 kyr, with a temporal resolution of 1–9 years depending on the depth. The EDC96 ice core, 788 m long, was drilled in the field seasons from 1996/97 to 1998/99 at Dome C, central East Antarctica ($75^{\circ}06' S$, $123^{\circ}24' E$; 3233 m a.s.l., about 1100 km from the coastline) in the framework of the EPICA programme. Ionic components (Na^+ , NH_4^+ , K^+ , Mg^{2+} , Ca^{2+} , Cl^- , NO_3^- , SO_4^{2-} , MSA) were measured by ion chromatography (IC) within the EPICA chemistry consortium, including laboratories from five European countries.

While the environmental and climatic significance of concentration changes of single components or component groups will be discussed in detail in specific papers, the aim of this paper is to give a first, preliminary overview of the pattern of all the analyzed compounds under the different climatic conditions spanning the last 45 kyr: the Holocene, the Holocene Optimum (HO), the last glacial/interglacial transition, the Last Glacial Maximum (LGM) and the Late-glacial period. Particular attention has been paid to evaluating the sensitivity of the potential environmental

markers to the climatic changes that occurred during the last transition, and especially during the Antarctic Cold Reversal (ACR; a mid-deglaciation cold episode indicated by a sharp decrease in the δD record starting from about 14.0 kyr BP; see section 3), by observing trends in their concentrations and fluxes. Moreover, the paper aims to check the reliability of concentration and flux profiles to provide information on changes in source intensity and transport efficiency of atmospheric aerosol and in snow accumulation rate.

2. METHODS

Data reported here come from IC analyses performed in different European laboratories on the entire EDC96 ice core. The core was drilled at Dome C as part of the EPICA programme aiming to reconstruct high-resolution isotopic, chemical and physical profiles for the last 1×10^6 years (EPICA Dome C 2001–02 Science and Drilling Teams, 2002). The first drilling attempt started during the 1996/97 campaign and stopped in 1998/99 because the drill got stuck at 788 m depth. This ice core was named EDC96. A second drilling, EDC99, started in the 1999/2000 field season and reached 3100 m depth, about 100 m above the bedrock, during the 2002/03 campaign. The two cores were analyzed in the field for electrical properties (ECM and dielectric profiling (DEP); Wolff and others, 1999; Udisti and others, 2000). While EDC99 chemical and isotopic analysis is still in progress, EDC96 measurements are almost complete along the entire core. IC analysis was performed on continuous ice-core sections in the framework of the EPICA chemical consortium, involving laboratories from Denmark, France, Italy, Sweden and the United Kingdom. Ice-core sections were decontaminated following two different approaches:

1. subsamples were cut by a stainless-steel saw and packed; in the European laboratories, ice pieces were decontaminated by mechanically removing (generally with an electric plane or by manual scraper) some millimetres of the external layer;
2. sections about 110 cm long (cross-section about 32 mm \times 34 mm) were continuously melted as described in Röthlisberger and others (2000a). The inner contaminant-free part of each bar was collected in pre-cleaned Coulter Counter-type accuvettes, subdividing the melted flux into subsamples with a sequential autosampler.

Ice-core cutting was performed at Dome C, while accuvette subsampling on the last 200 m was carried out at the Alfred Wegener Institute, Bremerhaven, Germany, in October 2000.

Subsamples have a resolution of 2.5–10 cm (corresponding to 1.0–4.0 and 2.2–9.0 years in the Holocene and in the glacial period, respectively), with the highest resolution in sections recording fast climatic changes (such as the transition, including the ACR).

Each laboratory received one in every five 55 cm sections, so that the accuracy of the measurements carried out by the different laboratories was continuously evaluated by comparison with the values measured on the contiguous sections. Inter-laboratory calibration rounds were periodically carried out to check the reliability of IC analysis and to tune analytical procedures and responses to obtain self-consistent profiles (Littot and others, 2002). Inter-laboratory

comparison carried out on standards at ppb levels and on Holocene samples, where the lowest concentrations were measured, yielded errors of <15%. Minimum errors (2.5%) were determined for sulphate, and maximum values (15%) for MSA and Mg. Very low Holocene levels of Ca, K and nitrate showed higher uncertainties (up to 50%), but these include errors in manipulation and transport of melted samples used for the inter-calibration exercise, while routine samples were decontaminated and analyzed from each laboratory just before the analysis. Glacial values were usually one to two orders of magnitude higher than the Holocene ones, so even the highest errors do not significantly affect the glacial-to-Holocene trends discussed here.

Firn sections showed high ammonium contamination by uptake of ammonia. In fact, the samples were stored in the Dome C buffer for >1 year (two field seasons), not sealed in polyethylene bags, because the analysis processing line was set up the year after drilling started. Ammonium data related to the first 100 m of the EDC96 ice core were discarded for the Holocene mean calculation.

ECM was performed on site (Wolff and others, 1999; Udisti and others, 2000). Isotopic δD measurements were carried out at Saclay, France, in the framework of the EPICA isotopes consortium (Jouzel and others, 2001).

Since the drilling site is located on the top of a dome, EDC96 dating (EDC1) was achieved by a simple flow model considering only vertical deformations and using accumulation-rate values calculated from the relationship between δD isotopic ratio and relative humidity; model parameters were calibrated by using volcanic signatures, the end of the Greenland Younger Dryas (YD; 11.53 kyr BP) and the ^{10}Be peak, occurring at 41 kyr BP (BP = before AD 1950), as temporal horizons (Schwander and others, 2001). The depth at EDC96 corresponding to the end of the YD has been estimated by isotope match (EDC96/Byrd: Hammer and others, 1994) and CH_4 match (Byrd/Greenland Icecore Project (GRIP): Blunier and others, 1998).

3. RESULTS AND DISCUSSION

Figure 1 shows the concentration/age profiles for all measured chemical species and ECM, contrasted to the δD profile for the last 45 kyr. On the basis of δD trends and the EDC1 time-scale, we divided the temporal range into five periods:

1. Holocene (without Climatic Optimum): 0–9.5 kyr BP; 6–300 m;
2. HO: 9.5–11.5 kyr BP; 300–360 m;
3. Transition: 11.5–18.0 kyr BP; 360–480 m;
4. LGM: 18.0–32.0 kyr BP; 480–640 m;
5. Glacial (part): 32.0–45.0 kyr BP; 640–780 m.

Vertical lines in Figure 1 separate the different periods.

During the glacial/interglacial transition, particular attention was paid to the ACR period (see section 3.3) and to the following warming phase until the beginning of the Holocene (about 11.5 kyr BP). The mid-deglaciation cold episode (ACR) is very evident in the δD record as a sharp decrease starting from about 14.0 kyr BP. The δD profile reaches a relative minimum value (end of ACR) at about 12.5 kyr BP. ACR climatic features and the temporal shift with respect to the Greenland YD have been discussed in several papers

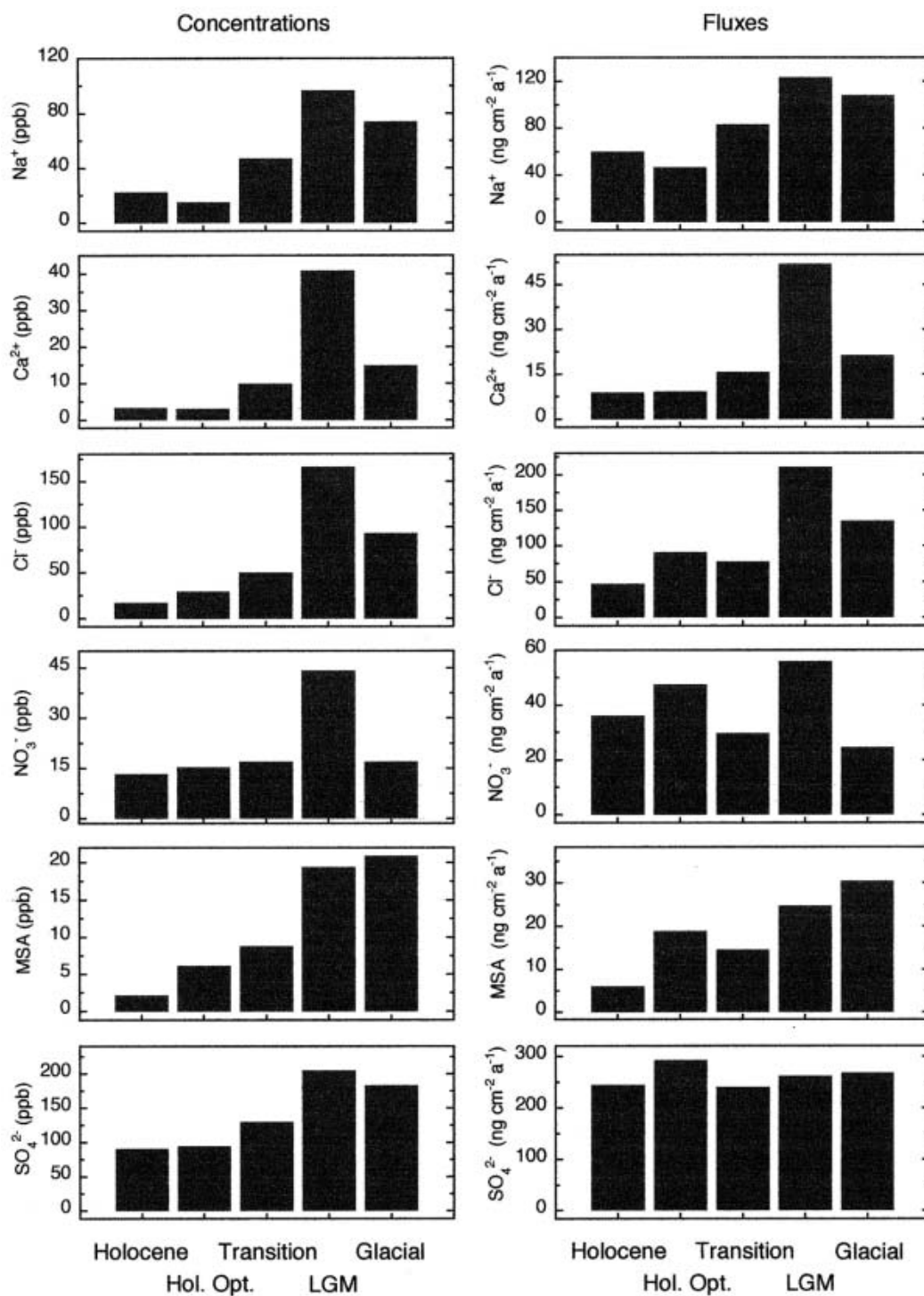


Fig. 2. Mean concentration (ppb) and flux ($\text{ng cm}^{-2} \text{a}^{-1}$) values for selected chemical species in the different climatic periods.

(see, e.g., Jouzel and others, 1995; Blunier and others, 1997).

As already pointed out by several authors (Legrand and others, 1988; Watanabe and others, 1999; Steig and others, 2000), background concentration values of chemical compounds show trends anticorrelated to the temperature, which is derived from the δD isotopic profile. We mainly refer to the warm events occurring around 42.5 and 38.0 kyr_{BP} (see δD peaks) and the following colder periods, to the LGM, to the transition and to the HO. The 38.0 kyr warm period was also found in the Byrd and Vostok ice cores and named A1 (Blunier and others, 1998). Another

older warm period, probably corresponding to the A2 warming event (Blunier and others, 1998), is partially recorded at the end of the EDC96 ice core.

Some components, such as Ca^{2+} , Cl^- , NO_3^- , Na^+ , Mg^{2+} and MSA, show high sensitivity to climatic changes (Fig. 1). Mean concentration values in the different climatic periods are reported in Figure 2. The highest concentrations were recorded in the cold periods, and especially in the LGM. Minimum background concentrations are observed in the warm stages of the glacial and in the Holocene. On the other hand, sulphate, ammonium, fluoride and, to a lesser extent, potassium, show minor changes in the different

climatic periods, with little variation also during the glacial/interglacial transition. As for ammonium, the mean concentration was calculated excluding the first 100 m, affected by contamination (see section 2).

Dome C past accumulation rates were calculated by supposing them to be proportional to the derivative of the mean saturation vapour pressure at the inversion layer with respect to temperature (Jouzel and others, 1987), where mean surface temperature was estimated from the stable-isotope ratio in the ice (Schwander and others, 2001). In this way, we reconstructed the accumulation-rate curve with a depth resolution of 0.55 m (corresponding to about 20 years in the Holocene and 50 years in the glacial). Since accumulation rate increases around 2.3 times from the LGM to the Holocene, we have to consider the effects of such changes on the snow content of the chemical compounds. On the basis of the EDC1 dating and taking into account the ice-layer thinning with depth, we associated to each concentration (C) the accumulation rate (A) evaluated for the time period covered by the sample resolution, calculating the net deposition fluxes (F):

$$F(\text{ng cm}^{-2} \text{ a}^{-1}) = C(\text{ng cm}^{-3}) \times A(\text{cm w.e. a}^{-1})$$

Both the use of concentration and the use of flux to study the temporal profiles of climatic and environmental markers along an ice core have advantages and disadvantages. Concentration is an independent chemical measurement and thus more reliable, but changes in concentration are dependent on variation in source intensity and transport efficiency as well as in accumulation rate, especially for sites where dry deposition is important or dominant (low-accumulation-rate areas, such as Dome C: Legrand, 1987). Flux (net deposition mass) is calculated by multiplying concentration by accumulation rate and is potentially affected by larger errors, mainly related to the reliable reconstruction of past accumulation rate from the isotopic profile. On the other hand, flux is virtually independent of accumulation rate at Dome C, dominated by dry-deposition processes, and therefore more suitable for assessing changes in atmospheric load. We use both parameters, preferring fluxes when studying the effects of source and transport changes, and concentrations when describing the comprehensive sensitivity (driven by accumulation rate, source and transport changes) of chemical profiles to climate variations.

3.1. Mean values

Figure 2 shows mean concentration and flux values for the most relevant components measured in the EDC96 ice core in the five different climatic stages.

The mean concentration general trends confirm the profile observations. The highest mean concentrations are measured in the LGM, when both temperature and accumulation rate were lower, and minimum values are recorded in the Holocene. This pattern is shown by Na^+ (Mg^{2+} and K^+ follow identical trends) and especially by Ca^{2+} , which exhibits the highest concentration change from high LGM values to minimum values during the HO. The parallelism between concentration and flux trends for Na^+ and Ca^{2+} demonstrates that accumulation rate tunes only the net deposition quantities but temporal changes are driven by sources and/or transport changes. By contrast, the variations observed in sulphate concentration trend practically disappear in the flux pattern, showing the sulphate deposition processes are almost completely dominated by changes in

accumulation rates. A small maximum is recorded during the HO, probably related to higher biogenic activity, as seems to be suggested by the contemporaneous increase in ammonium and MSA fluxes.

Chloride and nitrate show a more complex pattern, mainly because they are not conservative species (Wolff, 1996). Indeed, post-depositional processes (diffusion, redistribution, re-emission into the atmosphere and photochemical reactions) can alter the original snow composition at low-accumulation sites (Wagon and others, 1999; Röthlisberger and others, 2000a, 2002b; Traversi and others, 2000). The present Dome C accumulation rate of $2.7 \text{ cm w.e. a}^{-1}$ was reduced to about 50% in the LGM (Schwander and others, 2001), so post-depositional processes heavily affect the chloride and nitrate preservation in snow at this site. As one of the main post-depositional processes is related to re-emission of the volatile acidic species (HNO_3 and HCl) into the atmosphere, alkaline dust was able to fix higher concentrations of chloride and nitrate as non-volatile salts during the glacial period (Röthlisberger and others, 2000a, 2002b). Therefore, chloride and nitrate concentrations and fluxes are highly dependent on changes in both accumulation rate and snow acidity. Indeed, these two components show relatively high fluxes during the HO, when snow accumulation rate was so high as to preserve larger quantities, and in the LGM, when maximum dust atmospheric load (Delmonte and others, 2002a,b) fixed higher chloride and nitrate depositions as non-volatile salts. The better preservation of HCl deposition in the HO is also demonstrated by the Cl^-/Na^+ ratio which shows, in this period, a maximum mean value (2.2 w/w) in the last 45 kyr, significantly higher than the sea-water ratio (1.8 w/w). The pattern in the HO is similar to that measured in the present uppermost superficial layers at Dome C, showing the original contemporaneous deposition of NaCl and HCl was preserved by a relatively high accumulation rate (Traversi and others, 2000). In the glacial period, before the LGM, covered by the EDC96 ice core (32.0–45.0 kyr BP), the dust atmospheric load was much lower than in the LGM (Petit and others, 1999), and the accumulation rate similar (Schwander and others, 2001). This environmental situation was still suitable for preserving chloride depositions, but the low snow alkalinity was probably insufficient to compensate the negative effect of low accumulation on re-emission of HNO_3 . Indeed, nitrate mean flux shows the lowest values in the entire core. The higher sensitivity of nitrate to post-depositional re-emission into the atmosphere is also demonstrated by the pattern of present snow deposition at Dome C: nitrate concentration (and flux) quickly decreases from high superficial values (around 150 ppb) to very low background Holocene values (around a few ppb) in the first 100 cm of snow layers (Traversi and others, 2000).

MSA is also affected by post-depositional effects, consisting of migration and re-emission processes, complicating its use as a univocal marker of past biogenic activity changes (Wagon and others, 1999; Pasteur and Mulvaney, 2000; Delmas and others, 2003). Therefore, the net depositional fluxes of this component are also probably directly correlated to snow accumulation rate and alkaline dust content in the snow. Indeed, the pattern of MSA fluxes in the Holocene, HO, transition and LGM are very similar to those shown by chloride and nitrate. In the rest of the glacial, by contrast, MSA shows the highest mean flux and concentration values in all the last 45 kyr. Because the

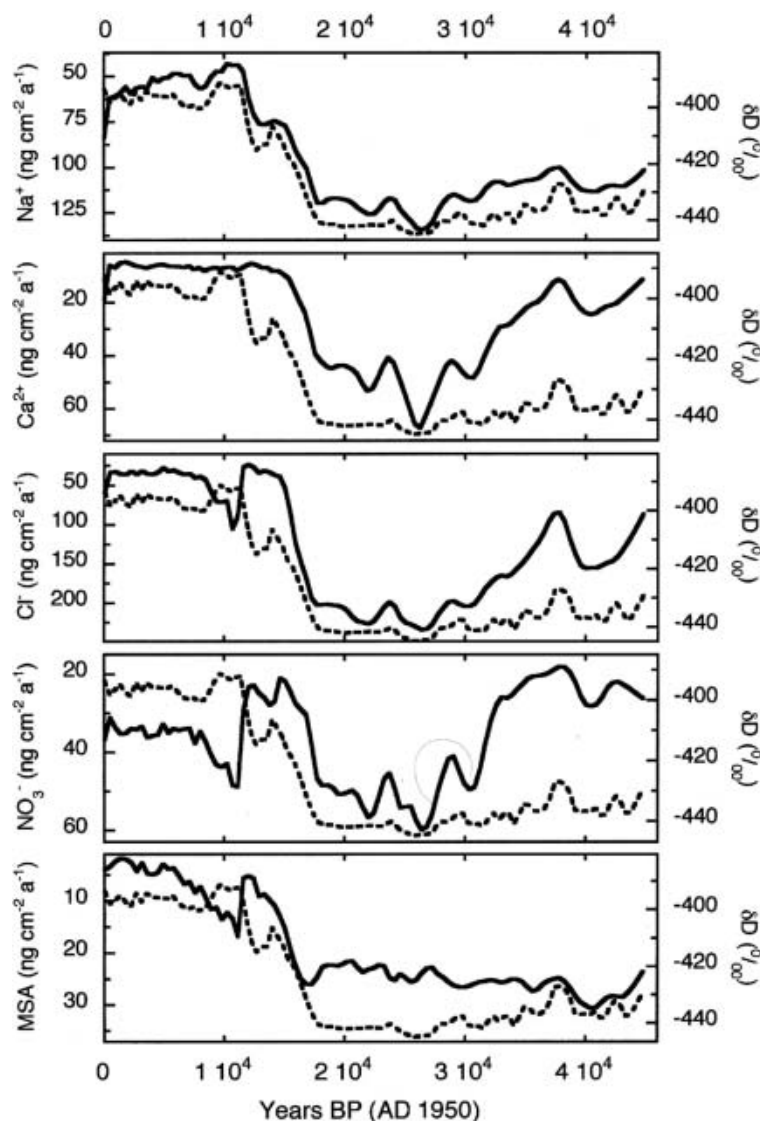


Fig. 3. Smoothed flux ($\text{ng cm}^{-2} \text{a}^{-1}$) stratigraphy of some chemical components, compared with the smoothed δD profile (dotted line), along the last 45 kyr. The smoothed fluxes are plotted on a reversed scale. See text for details of smoothing procedure.

32.0–45.0 kyr_{BP} glacial period was characterized by low alkaline-dust atmospheric load and snow accumulation rates, we postulate that the highest MSA fluxes with respect to the LGM reflect higher phytoplanktonic activity or more efficient meridional transports from oceanic area sources of biogenic emissions or a different oxidation pathway of phytoplanktonic dimethylsulphide, producing a higher MSA/H₂SO₄ ratio.

3.2. Flux profiles

The flux patterns observed from multi-millennial averages can be observed in detail by continuous 45 kyr profiles. Figure 3 shows the smoothed trends of the Na⁺, Ca²⁺, Cl⁻, NO₃⁻ and MSA fluxes, compared with the smoothed δD profile. The smoothing procedure was made by a weighted fitting curve. This function fits a curve to the data using a locally weighted least-squares error method. The result of this curve fit is to plot a best-fit smooth curve through the centre of the data. This is a robust fitting technique, nearly insensitive to outliers, and so able to give a reliable trend for background values. The low percentage of the smoothing (2% for δD and 3% for chemical profiles) ensures a sufficient

temporal resolution for the interval, around each value, where smoothing was carried out (for the chemical dataset, 3% = 600 values). The running procedure restitutes a number of values as high as the original dataset.

To indicate the general inverse relationship and the particular features of the different profiles with respect to the isotopic profile, we use an unusual presentation, plotting the flux profiles in a reversed scale. In this way, the anticorrelation between chemical and isotopic profiles during warm and cold stages and transition appears as parallel trends, indicating particular patterns in the ACR.

In the Na⁺ and Ca²⁺ flux profiles, the inverse relationship between fluxes and isotopic temperature is very evident. All climatic changes (warm and cold stages in the glacial period, LGM, transition, ACR, HO) are recorded in the Na⁺ profile, indicating an anticorrelation between source intensity or transport efficiency and temperature in the different climatic periods. Ca²⁺ shows a still higher sensitivity for the A1 stage and, especially, for the LGM, when high atmospheric dust levels increase the depositional Ca²⁺ fluxes. Unlike Na⁺, however, Ca²⁺ exhibits no significant change during the ACR and the entire Holocene,

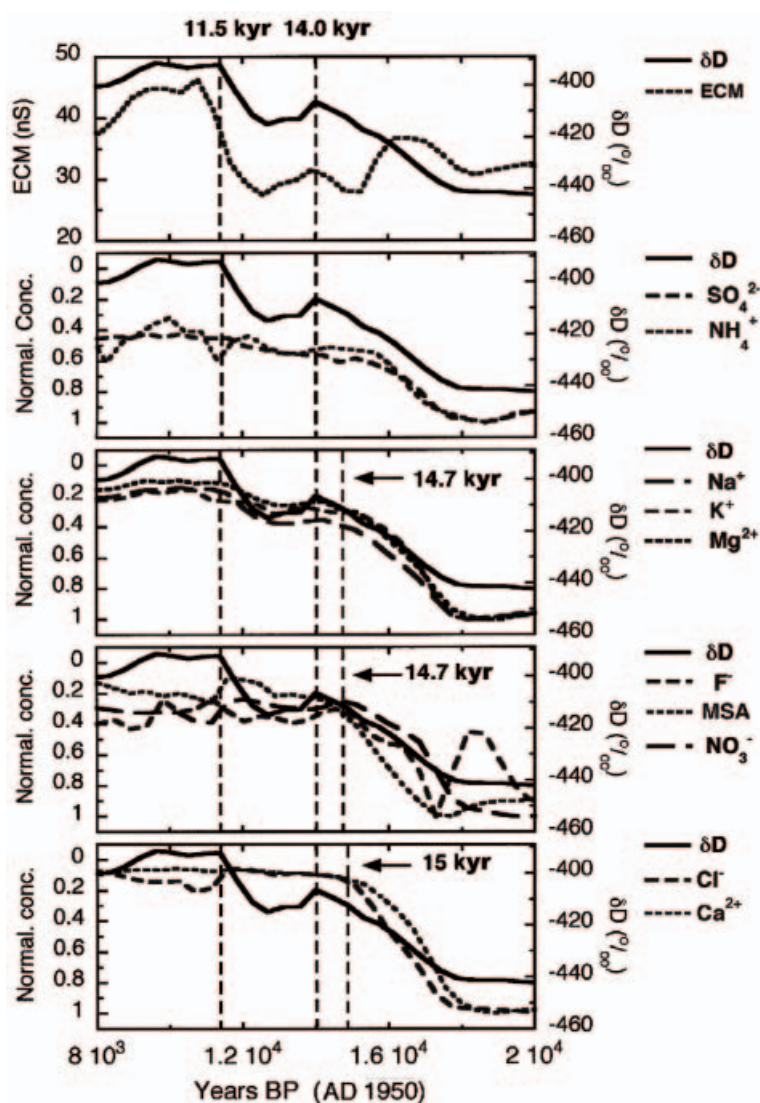


Fig. 4. Smoothed normalized concentration profiles of all the measured components during the last transition (8.0–20 kyr BP), superimposed on the δD profile. Smoothed normalized concentrations are plotted on a reversed scale. See text for normalization and smoothing procedures.

demonstrating a different pattern of the dust source areas, with respect to sea spray, during the transition (see further below). Na^+ sensitivity with respect to the ACR climate oscillation could be related to change in atmospheric transport processes, probably driven by redistribution of the latitudinal temperature gradient. Similar trends were observed by R othlisberger and others (2002a) using non-sea-salt Ca^{2+} (nssCa^{2+}) and sea-salt Na^+ (ssNa^+) flux profiles obtained by continuous flow analysis (CFA; R othlisberger and others, 2000b). For the ssNa^+ profile, however, these authors did not discuss the situation of the ACR. Here, we preferred to use total Ca^{2+} and Na^+ flux profiles to avoid every potential artefact in the original trends. Anyway, as the Ca^{2+} drops to very low fluxes about 1.0 kyr before the ACR onset (see section 3.3), the crustal contribution to the Na^+ budget is only few per cent and is not sufficient to affect the observed trend.

The chloride and nitrate trends during the glacial and early transition fit the Ca^{2+} pattern very well, confirming the role of alkaline dust in fixing them in the snow layers as non-volatile salts. In particular, the nitrate profile is nearly superimposable on that of Ca^{2+} during the early transition

(see, for detail, Fig. 4), in the LGM and in the rest of the glacial (with some differences in the deepest part of the ice core), showing the same sensitivity to warm and cold stages. Conversely, chloride and nitrate fluxes differ from Ca^{2+} in the late transition and early Holocene. Here also, nitrate has the highest sensitivity to climatic changes, showing a sharp increase in the net deposition flux in phase (Figure 3 reports fluxes as reversed scale) with temperature maxima at the ACR onset (about 14.2 kyr BP) and in the HO, probably driven by the accumulation-rate increases and not by dust content (Ca^{2+} fluxes are very low in the same time periods). A flux peak during the HO is also visible in the chloride profile, while no significant changes are seen in the ACR. The MSA profile is characterized by high, constant fluxes during the LGM and glacial, with low sensitivity, sometimes out of phase, to isotopic temperature changes. An inverse relationship is shown during the warm stages in the glacial, especially during A1. No significant changes are visible during the ACR, while a sharp flux increase occurs in the HO, with the same relative intensity as chloride. Finally, a progressive decreasing trend of MSA fluxes is evident during the Holocene, reaching relative stability in the last 5 kyr.

3.3. Temporal dephasing during the transition

Figure 4 shows the concentration profiles of some of the measured components during the transition, compared to δD and ECM profiles. Concentrations are plotted on a reversed scale as smoothed normalized profiles. The normalization was obtained for each component by dividing each sample concentration by the highest value measured for the same components during the LGM (when all components show maximum concentrations). Here, we preferred to report concentration instead of fluxes, to avoid any possible artefact due to an incorrect evaluation of snow accumulation rate in a temporal range where climatic changes were very fast. Besides, as already noted, concentration variations could be more suitable for evaluating the overall climate sensitivity of a snow component, including the effects of accumulation-rate changes as well as source and transport variations. Also in this case, the inverse scale allows easier comparison with the isotopic profile, better indicating changes in each profile slope.

Although ECM is mainly related to snow background acidity (Hammer and others, 1980), it also depends on the ionic content so that the smoothed ECM profile shows a different pattern with respect to the other considered parameters. For the Holocene, Barnes and others (2002) found a difference between the calculated acidity from H_2SO_4 , HCl and HNO_3 and that resulting from simple models of electrical measurements; the authors hypothesize that with a larger grain-size a greater connectivity occurs with the same amount of acid, and therefore higher conductivity results. In the glacial period the issue is more complex due to the high dust content, and further investigation is needed to fully understand the electric signals.

The majority of chemical components parallel the isotopic curve up to the ACR, showing an inverse relationship between concentration and temperature. Starting from the ACR onset, concentrations tend to reach the low Holocene values with a much slower gradient, revealing a general low sensitivity for the ACR oscillation and HO conditions. Two groups of chemical components show a quite different pattern. On the one hand, sulphate and ammonium reversed profiles follow, perfectly in phase, the δD profile up to reach the low, quite constant, Holocene values about 1.6 kyr before the ACR onset, which occurred about 14.0 kyr ago (Schwander and others, 2001). On the other hand, nitrate and Ca^{2+} reversed concentration profiles precede the isotopic transition onset by about 300 years, with a dephasing very similar to that shown by ECM. After the first abrupt increase, nitrate and Ca^{2+} reach the low Holocene values about 1.0 kyr before the ACR onset, similarly to chloride. Whereas Ca^{2+} and chloride show no significant changes in the second step of the deglaciation, nitrate exhibits a concentration increase whose relative maximum is in phase with the ACR onset.

The pattern of Na^+ (very similar to those shown by Mg^{2+} and K^+) is different: the inverse normalized concentration fits the δD profile very well, following the ACR oscillation. Only MSA, of the components analyzed, shows a long delay (about 400 years) with respect to the δD increase in the deglaciation onset.

Finally, the large fluoride peak during the LGM is due to the 170 year fluoride event first identified by Hammer and others (1997) in the Byrd ice core.

4. CONCLUSIONS

Granting concentrations can reliably describe the comprehensive environmental changes that occurred during the last deglaciation, the study of the high-resolution chemical trends revealed that environmental changes in the aerosol source areas preceded or were contemporaneous (with the apparent exceptions of chloride and, especially, MSA) to the Antarctic temperature changes, as evaluated by the δD isotopic profile. This probably implies that the Antarctic site temperature (as recorded at Dome C) did not lead changes in the snow deposition composition, except for variations in the snow accumulation rates.

In particular, the Ca^{2+} decrease before the deglaciation onset, in phase with the acidity increase (as revealed by the ECM profile), shows that the main dust-source areas for east central Antarctica (Patagonia: Basile and others, 1997) experienced environmental variations in advance of central Antarctic temperature changes. R othlisberger and others (2002a) suggested that the early Ca^{2+} decrease could be related to changes in Patagonian climatic conditions (warmer temperature and higher humidity leading to larger vegetation growth) during the last part of the LGM (McCulloch and Davies, 2001). Unfortunately, the oldest record reported by these authors dates back to 17.33 kyr BP, while the isotopic temperature at Dome C increases from around 18.0 kyr BP, so that we have no definite evidence the Patagonian warming started in advance. Anyway, the Ca^{2+} profile trend suggests that dust-source areas affecting Dome C snow deposition started to warm a few hundred years before east central Antarctic warming and probably reached environmental conditions leading to low dust production (larger humidity and vegetation cover: McCulloch and Davies, 2001; R othlisberger and others, 2002a) around 1 kyr before the ACR. The dating of the Ca^{2+} stabilization, around 15.0 kyr BP, is congruous with the McCulloch and Davies (2001) observation that southern Patagonia was humid from 16.91 kyr BP. As pointed out by R othlisberger and others (2002a), it remains unknown why the re-establishment of dry, cold conditions in Patagonia, from 15.33 kyr BP (McCulloch and Davies, 2001), was not recorded in the Ca^{2+} Dome C profile. Changes in atmospheric circulation, driven by the lower Equator-to-pole temperature gradient and the increased effect of zonal circulation, with respect to meridional transport (Delmonte and others, 2002a), could explain this pattern. Analogous explanations could help in understanding the pattern of Na^+ and other chemical components showing high sensitivity to the second warming step and the HO conditions (see flux profiles in Fig. 3).

Mainly snow accumulation-rate changes could affect, on the other hand, sulphate and ammonium snow content (with some possible exception during the HO), as observed from the concentration and fluxes along the EDC96 ice core.

Finally, the question of which process has driven the acid/base equilibrium of snow during the transition cannot be reliably answered from the chemical profile. Indeed, ECM shows the highest increase in the second step of the transition, after all chemical components reached low Holocene levels.

The observation of several previous deglaciation periods, recorded in the new EDC99 ice core, will allow confirmation of the observed environment–climate relationships and a better understanding of the factors controlling snow acidity.

ACKNOWLEDGEMENTS

This work is a contribution to the 'European Project for Ice Coring in Antarctica' (EPICA), a joint European Science Foundation (ESF)/European Commission (EC) scientific programme, funded by the European Commission and by national contributions from Belgium, Denmark, France, Germany, Italy, the Netherlands, Norway, Sweden, Switzerland and the United Kingdom. This is EPICA publication No. 75. The research was partially supported by Ente per le Nuove Tecnologie, l'Energia e l'Ambiente (ENEA) through a cooperation agreement with the Universities of Milan-Bicocca and Venice, in the framework of the 'Glaciology' and 'Chemical Contamination' sections of Programma Nazionale di Ricerche in Antartide (PNRA).

REFERENCES

- Barnes, P. R. F., E. W. Wolff, R. Udisti, E. Castellano, R. Röthlisberger and J. P. Steffensen. 2002. The effect of density on electrical conductivity of chemically laden polar ice. *J. Geophys. Res.*, **107**(B2), 2029. (10.1029/2000JB000080.)
- Basile, I., F. E. Grousset, M. Revel, J. R. Petit, P. E. Biscaye and N. I. Barkov. 1997. Patagonian origin of glacial dust deposited in East Antarctica (Vostok and Dome C) during glacial stages 2, 4 and 6. *Earth Planet. Sci. Lett.*, **146**(3–4), 573–589.
- Blunier, T. and 9 others. 1997. Timing of the Antarctic cold reversal and the atmospheric CO₂ increase with respect to the Younger Dryas event. *Geophys. Res. Lett.*, **24**(21), 2683–2686.
- Blunier, T. and 10 others. 1998. Asynchrony of Antarctic and Greenland climate change during the last glacial period. *Nature*, **394**(6695), 739–743.
- Cole-Dai, J., E. Mosley-Thompson, S. P. Wight and L. G. Thompson. 2000. A 4100-year record of explosive volcanism from an East Antarctic ice core. *J. Geophys. Res.*, **105**(D19), 24,431–24,441.
- Delmas, R. J., S. Kirchner, J. M. Palais and J.-R. Petit. 1992. 1000 years of explosive volcanism recorded at the South Pole. *Tellus*, **44B**(4), 335–350.
- Delmas, R. J., P. Wagnon, K. Goto-Azuma, K. Kamiyama and O. Watanabe. 2003. Evidence for the loss of snow-deposited MSA to the interstitial gaseous phase in central Antarctic firn. *Tellus*, **55B**(1), 71–79.
- Delmonte, B., J.-R. Petit and V. Maggi. 2002a. Glacial to Holocene implications of the new 27000-year dust record from the EPICA Dome C (East Antarctica) ice core. *Climate Dyn.*, **18**(8), 647–660. (10.1007/s00382-001-0193-9.)
- Delmonte, B., J.-R. Petit and V. Maggi. 2002b. LGM–Holocene changes and Holocene millennial-scale oscillations of dust particles in the EPICA Dome C ice core, East Antarctica. *Ann. Glaciol.*, **35**, 306–312.
- Dentener, F. J. and P. J. Crutzen. 1994. A tri-dimensional model of the global ammonia cycle. *J. Atmos. Chem.*, **19**, 331–369.
- EPICA Dome C 2001–02 Science and Drilling Teams. 2002. Extending the ice core record beyond half a million years. *Eos*, **83**(45), 509, 517.
- Hammer, C. U., H. B. Clausen and W. Dansgaard. 1980. Greenland ice sheet evidence of post-glacial volcanism and its climatic impact. *Nature*, **288**(5788), 230–235.
- Hammer, C. U., H. B. Clausen and C. C. Langway, Jr. 1994. Electrical conductivity method (ECM) stratigraphic dating of the Byrd Station ice core, Antarctica. *Ann. Glaciol.*, **20**, 115–120.
- Hammer, C. U., H. B. Clausen and C. C. Langway, Jr. 1997. 50,000 years of recorded global volcanism. *Climatic Change*, **35**(1), 1–15.
- Hansson, M. E. and E. S. Saltzman. 1993. The first Greenland ice core record of methanesulfonate and sulfate over a full glacial cycle. *Geophys. Res. Lett.*, **20**(12), 1163–1166.
- Jouzel, J. and 6 others. 1987. Vostok ice core: a continuous isotope temperature record over the last climatic cycle (160,000 years). *Nature*, **329**(6138), 403–408.
- Jouzel, J. and 11 others. 1995. The two-step shape and timing of the last deglaciation. *Climate Dyn.*, **11**(3), 151–161.
- Jouzel, J. and 12 others. 2001. A new 27 kyr high resolution East Antarctic climate record. *Geophys. Res. Lett.*, **28**(16), 3199–3202.
- Legrand, M. 1987. Chemistry of Antarctic snow and ice. *J. Phys.* (Paris), **48**, Colloq. C1, 77–86. (Supplément au 3.)
- Legrand, M. R., C. Lorius, N. I. Barkov and V. N. Petrov. 1988. Vostok (Antarctica) ice core: atmospheric chemistry changes over the last climatic cycle (160,000 years). *Atmos. Environ.*, **22**(2), 317–331.
- Legrand, M., C. Feniet-Saigne, E. S. Saltzman, C. Germain, N. I. Barkov and V. N. Petrov. 1991. Ice-core record of oceanic emissions of dimethylsulphide during the last climate cycle. *Nature*, **350**(6314), 144–146.
- Legrand, M. and 6 others. 1997. Sulfur-containing species (methanesulfonate and SO₄) over the last climatic cycle in the Greenland Ice Core Project (central Greenland) ice core. *J. Geophys. Res.*, **102**(C12), 26,663–26,679.
- Legrand, M., F. M. Ducroz, D. Wagenbach, R. Mulvaney and J. Hall. 1998. Ammonium in coastal Antarctic aerosol and snow: role of the polar ocean and penguin emissions. *J. Geophys. Res.*, **103**(D9), 11,043–11,056.
- Littot, G. C. and 9 others. 2002. Comparison of analytical methods used for measuring major ions in the EPICA Dome C (Antarctica) ice core. *Ann. Glaciol.*, **35**, 299–305.
- Mayewski, P. A. and M. Legrand. 1990. Recent increase in nitrate concentration of Antarctic snow. *Nature*, **346**(6281), 258–260.
- McCulloch, R. D. and S. J. Davies. 2001. Late-glacial and Holocene palaeoenvironmental change in the central Strait of Magellan, southern Patagonia. *Palaeogeogr., Palaeoclimatol., Palaeoecol.*, **173**(3–4), 143–173.
- Pasteur, E. C. and R. Mulvaney. 2000. Migration of methane sulphonate in Antarctic firn and ice. *J. Geophys. Res.*, **105**(D9), 11,525–11,534.
- Petit, J.-R. and 18 others. 1999. Climate and atmospheric history of the past 420,000 years from the Vostok ice core, Antarctica. *Nature*, **399**(6735), 429–436.
- Röthlisberger, R., M. A. Hutterli, S. Sommer, E. W. Wolff and R. Mulvaney. 2000a. Factors controlling nitrate in ice cores: evidence from the Dome C deep ice core. *J. Geophys. Res.*, **105**(D16), 20,565–20,572.
- Röthlisberger, R. and 6 others. 2000b. Technique for continuous high-resolution analysis of trace substances in firn and ice cores. *Environ. Sci. Technol.*, **34**(2), 338–342.
- Röthlisberger, R. and 6 others. 2002a. Dust and sea salt variability in central East Antarctica (Dome C) over the last 45 kyrs and its implications for southern high-latitude climate. *Geophys. Res. Lett.*, **29**(20), 1963. (10.1029/2002GL015186.)
- Röthlisberger, R. and 10 others. 2002b. Nitrate in Greenland and Antarctic ice cores: a detailed description of post-depositional processes. *Ann. Glaciol.*, **35**, 209–216.
- Ruth, U., D. Wagenbach, M. Bigler, J. P. Steffensen, R. Röthlisberger and H. Miller. 2002. High-resolution microparticle profiles at NorthGRIP, Greenland: case studies of the calcium–dust relationship. *Ann. Glaciol.*, **35**, 237–242.
- Schwander, J., J. Jouzel, C. U. Hammer, J. R. Petit, R. Udisti and E. Wolff. 2001. A tentative chronology for the EPICA Dome Concordia ice core. *Geophys. Res. Lett.*, **28**(22), 4243–4246.
- Steig, E. J. and 7 others. 2000. Wisconsinan and Holocene climate history from an ice core at Taylor Dome, western Ross Embayment, Antarctica. *Geogr. Ann.*, **82A**(2–3), 213–235.
- Stenni, B. and 7 others. 2001. An oceanic cold reversal during the last deglaciation. *Science*, **293**(5537), 2074–2077.
- Traversi, R., S. Becagli, E. Castellano, O. Largiuni and R. Udisti. 2000. Stability of chemical species in firn layers from Antarctica. In Colacino, M. and G. Giovannelli, eds. *8th Workshop, Italian*

- Research on the Antarctic Atmosphere. Proceedings. Vol. 69.* Bologna, Società Italiana di Fisica, 421–443.
- Udisti, R. and 6 others. 2000. Holocene electrical and chemical measurements from the EPICA–Dome C ice core. *Ann. Glaciol.*, **30**, 20–26.
- Vimeux, F., K. M. Cuffey and J. Jouzel. 2002. New insights into Southern Hemisphere temperature changes from Vostok ice cores using deuterium excess correction. *Earth Planet. Sci. Lett.*, **203**(3–4), 829–843.
- Wagnon, P., R. J. Delmas and M. Legrand. 1999. Loss of volatile acid species from upper firn layers at Vostok, Antarctica. *J. Geophys. Res.*, **104**(D3), 3423–3431.
- Watanabe, O., K. Kamiyama, H. Motoyama, Y. Fujii, H. Shoji and K. Satow. 1999. The palaeoclimate record in the ice core from Dome Fuji station, Antarctica. *Ann. Glaciol.*, **29**, 176–178.
- Wolff, E. W. 1995. Nitrate in polar ice. In Delmas, R. J., ed. *Ice core studies of global biogeochemical cycles*. Berlin, etc., Springer-Verlag, 195–224. (NATO ASI Series I: Global Environmental Change 30.)
- Wolff, E. W. 1996. Location, movement and reactions of impurities in solid ice. In Wolff, E. W. and R. C. Bales, eds. *Chemical exchange between the atmosphere and polar snow*. Berlin, etc., Springer-Verlag, 541–560. (NATO ASI Series I: Global Environmental Change 43.)
- Wolff, E., I. Basile, J.-R. Petit and J. Schwander. 1999. Comparison of Holocene electrical records from Dome C and Vostok, Antarctica. *Ann. Glaciol.*, **29**, 89–93.
- Zielinski, G. A. 2000. Use of paleo-records in determining variability within the volcanism–climate system. *Quat. Sci. Rev.*, **19**(1–5), 417–438.